Available online at www.sciencedirect.com
SCIENCE DIRECT®
ELSEVIER
International Journal of Solids and Structures 43 (2006) 5228–5246
INTERNATIONAL JOURNAL OF SOLIDS and STRUCTURES
www.elsevier.com/locate/ijsolstr

Mechanical behavior of sandwich panels with tetrahedral and Kagome truss cores fabricated from wires

Ji-Hyun Lim, Ki-Ju Kang *

Department of Mechanical Engineering, Chonnam National University, 300 Yongbongdong, Bukku, Kwangju 500-757, Republic of Korea

Received 20 April 2005; received in revised form 4 July 2005
Available online 16 September 2005

Abstract

Wires are great candidates as the raw material for truss periodic cellular metals because they can display high strength as in piano wires, are easy to fabricate, and can be controlled to be defect free. New approaches based on tri-axial weaving of wires to create ideal trusses, i.e., tetrahedral and Kagome truss have been presented. The mechanical properties of the sandwich panels with the truss cores fabricated by using the new approaches under compression and bending loadings are analyzed by elementary beam theory and experiments. The relative density, stiffness, and strength of the sandwich panels are estimated by the derived equations and compared with the measured results. The failure mechanisms of the sandwich panels are analyzed, and also benefits and shortcomings of each approach with respect to mechanical performance and production are discussed.
© 2005 Elsevier Ltd. All rights reserved.

Keywords: Truss PCM; Kagome truss; Tetrahedral truss; Sandwich panel; Tri-axial weaving; Failure mechanisms

1. Introduction

Since the new millennium, truss PCMs (periodic cellular metals) have drawn attention because of their high multi-functionality, which mostly due to the open cell architecture, as well as their excellent specific strength and stiffness. Several types of trusses are available; pyramid, lattice block, tetrahedral (or octet), Kagome and so on. A number of mechanical analyses on the truss PCMs have been performed.

For the tetrahedral or octet truss PCM, Deshpande et al. (2001) have investigated elastic properties and yield surface of the bulk material, and subsequently have researched the collapse mechanism of sandwich

* Corresponding author. Tel.: +82 62 5301668; fax: +82 62 5301689.
E-mail address: kjkang@chonnam.ac.kr (K.-J. Kang).

0020-7683/$ - see front matter © 2005 Elsevier Ltd. All rights reserved.
doi:10.1016/j.ijsolstr.2005.07.011

panels with one layer of tetrahedral truss core (Deshpande and Fleck, 2001). Wicks and Hutchinson (2001, 2004) have estimated the strength of sandwich panels for competing failure mechanisms. They also addressed the optimization of the sandwich panels subjected to crushing stress, bending, and transverse shear. Chiras et al. (2002) have developed an analytic model of the deformation of panel under shear loading and a Timoshenko-type theory for deformation of a panel with a truss core under three-point bending. Rathbun et al. (2004) have shown that finite element method can be used to successfully simulate the collapse behavior of sandwich panels with truss core under shear and bending loads.

For the lattice block structure PCM, Wallach and Gibson (2001a) have investigated the elastic moduli and strength of under compression and shear load. Also, Zhou et al. (2004) have investigated the deformation behavior of the lattice block structure PCM under compression. Both works carried out experiments in parallel with numerical methods.

For Kagome truss PCM, Hyun et al. (2003) have shown that the isotropy and stability of plastic deformation of Kagome truss PCM under compression and shear loading are superior to those of octet truss by finite element simulations. Wang et al. (2003) demonstrated the same benefits through experiments.

Initially, because of the complex shape, all of the specimens were made by investment casting assisted by rapid prototyping techniques (Chiras et al., 2002). Consequently, only metals with good castibility were selected: castable aluminum alloys (Wallach and Gibson, 2001a,b; Zhou et al., 2004; Sugimura, 2004; Deshpande and Fleck, 2001; Deshpande et al., 2001), copper/beryllium alloy (Chiras et al., 2002; Wang et al., 2003), and silicon brass (Deshpande and Fleck, 2001). Also, the truss specimens had low strength because the cast structures contained many intrinsic defects, which led to brittle failure of struts composing the truss, i.e., low strength. Moreover, low productivity and high cost were inevitable. As an alternative, Sypeck and Wadley (2002) proposed that the tetrahedral trusses could be fabricated from wrought metals by starting with perforated metal sheets and bending them along diagonal nodes. The trusses could then serve as a core, bonded with thin metal face sheets by brazing to create a sandwich panel or they could be stacked node-to-node and bonded to create a bulk material. The product is likely to be more robust owing to the wrought nature of the material as well as cost effective. However, material loss is unavoidable and local tearing or wrinkling could happen depending on the material when punching is involved in the perforation process. The same researchers (Sypeck and Wadley, 2001) have proposed an even cheaper fabrication process, in which metal textiles are layered and bonded to create a bulk material. Even though this can be considered as a truss PCM, the unit cell is square on two sides, pyramidal on the other two sides, and rectangular on the remaining sides, which do not form an ideal truss. Therefore, the specific strength is likely to be inferior. They also have proposed a new process in which metal textiles (Wadley et al., 2003) or expanded metals (Wadley, 2002) containing a square array of holes are bent along diagonal nodes to create pyramidal trusses. Jung et al. (2004) have successfully applied electric resistance welding as a bonding process for mass production of the sandwich panels having a pyramidal truss core formed from expanded metals. Recently, Queheillalt and Wadley (2005) have reported a simple method which involves layering a collinear array of either solid wires or tubes, alternating the direction of successive layers, and brazing.

In this work, wires are thought to be the best candidate material to create truss PCMs, because they can easily obtain high strength as in piano wires, are simple to fabricate, and can be controlled for good quality. However, the methods reported to date that use wires produce only PCMs with non-ideal trusses such as the structure of layering textiles (Sypeck and Wadley, 2001), pyramidal truss (Wadley et al., 2003; Wallach and Gibson, 2003), and simple square lattice (Queheillalt and Wadley, 2005). In this work, the authors present new approaches based on tri-axial weaving of wires to create ideal trusses, i.e., tetrahedral and Kagome truss. Wallach and Gibson (2003) have taken a similar approach, in which wires are bent into triangular wave shape and then inter-woven to form the truss configuration. But the differences between their approach and ours are obvious. In their approach, the wires are woven in two directions like warp and weft in an ordinary textile to form pyramidal trusses. The mechanical properties of sandwich panels with the truss cores fabricated using the new approaches under compression and bending load are analyzed by

elementary beam theory and experiments. The failure mechanism, which has never been reported before, and also benefits and shortcomings of the new approach from a practical viewpoint are discussed.

2. Design and fabrication

2.1. Tetrahedral truss core sandwich panel

Fig. 1(a) shows a typical sandwich panel with the tetrahedral truss core. In this work, a new approach has been used to form the core. First, wires are bent into a triangular wave shape shown in Fig. 2(a), and then, are assembled together as shown in Fig. 2(b)–(d). Each strut is composed of two parallel wires. At every apex, three wires pass by each other with little interference (see the inset in Fig. 2(d) for enlarged image). Fig. 3 is a top view of Fig. 2(d). One wire of a strut hides beneath the other, and three wires overlap each other clockwise (or counter-clockwise) at an apex. Finally, two face sheets are bonded on the top and bottom of the truss core to form a sandwich panel.

The theoretical strength and stiffness of the panel are given as follows. Here, it is assumed that the total thickness of the panel, D is much larger than the thickness of the face sheets, t_f, or that of the wires, d, i.e., $D \gg t_f$, d. Two kinds of the face sheets are considered: perforated sheets and solid face sheets. Fig. 4 illustrates the perforated face sheet. If the material of the face sheets is the same as that of the cores, the relative density of the panel with the perforated face sheet and the one with the solid face sheet are

$$\rho = \frac{6\sqrt{2}wt_f}{l^2} + \frac{3\sqrt{2}\pi d^2}{2l^2} \quad \text{and} \quad \rho = \frac{\sqrt{6}t_f}{l} + \frac{3\sqrt{2}\pi d^2}{2l^2}, \tag{1}$$

respectively, where w is the in-plane thickness of the bars composing the perforated face sheet as shown in Fig. 4. The first and second terms correspond to the face sheets and the core, respectively.

When a compressive force, p and a shear force, q are applied on the top of the unit tetrahedral truss composed with two wires for each strut as shown in Fig. 5(a) and (b), according to Castigliano's second theorem (Gere, 2001), the stiffness is given by

$$\frac{p}{\delta_p} = \frac{\pi d^2 E_c}{l} \quad \text{and} \quad \frac{q}{\delta_q} = \frac{\pi d^2 E_c}{4l}, \tag{2}$$

respectively, where δ_p and δ_q are the displacements corresponding to p and q, respectively, and E_c is the Young's modulus of the core material. From Eq. (2), the effective Young's modulus in the direction-3, E_{33} and shear modulus, G_{13} of the tetrahedral truss core are derived as

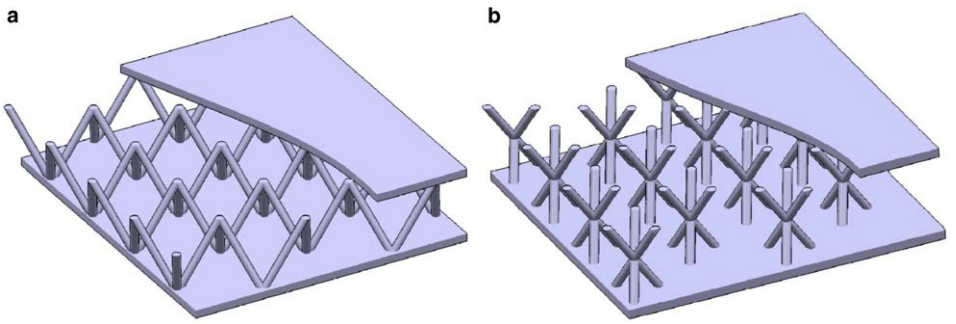

Fig. 1. Structure of typical sandwich panels with (a) tetrahedral truss core and (b) Kagome truss core.

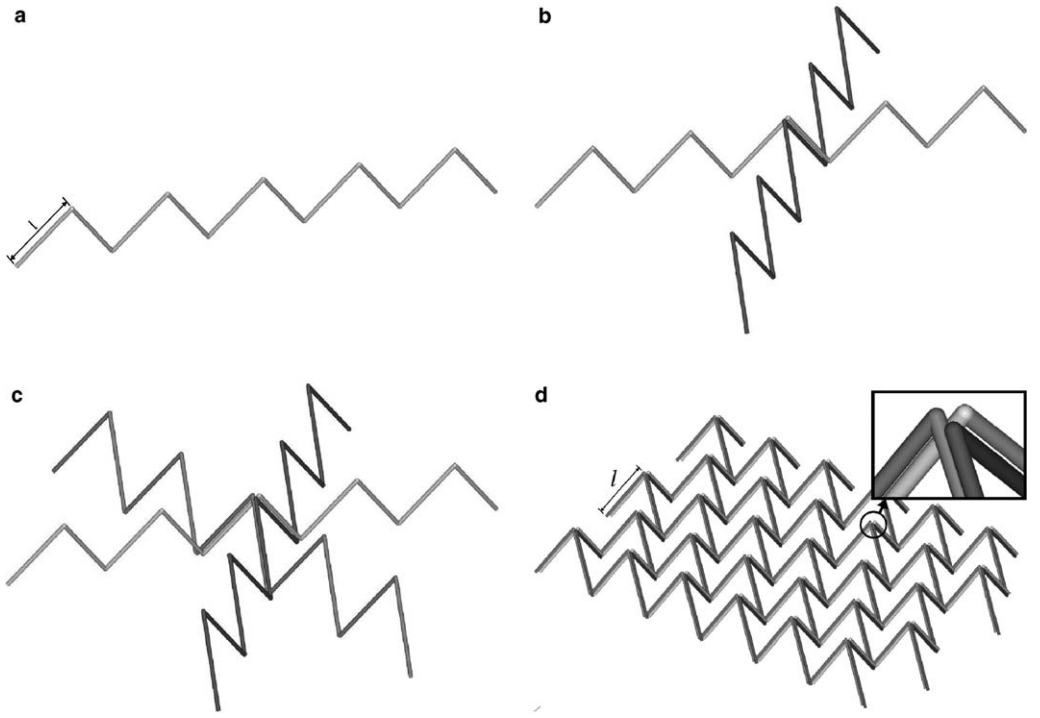

Fig. 2. Fabrication process of a tetrahedral sandwich panel with wires: (a) unit wire composing the truss, (b) two wires crossing each other, (c) three crossed wires where the junction builds a tetrahedral truss, (d) fully assembled truss, where the inset shows how the wires pass one other near the peak.

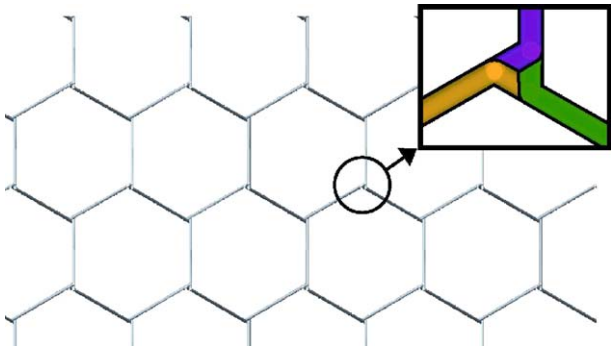

Fig. 3. Top view of the tetrahedral core shown in Fig. 2.

$$E_{33} = \frac{2\sqrt{2}\pi}{3} E_c \left(\frac{d}{l}\right)^2, \qquad G_{13} = \frac{\sqrt{2}\pi}{6} E_c \left(\frac{d}{l}\right)^2. \tag{3}$$

When the panel is to be tested under bending load as shown in Fig. 6(a), the external force and reactions are applied via the thick rigid blocks, each of which has a concave surface on one side, to prevent the panel from indentation. While the block at the both ends can rotate freely, the block at the center can not rotate because of the symmetry as long as the materials deform elastically. (Asymmetric deformation after yielding

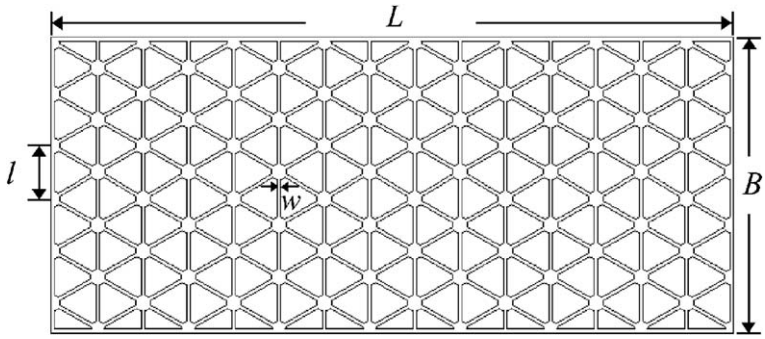

Fig. 4. Configuration of a perforated face sheet for the tetrahedral truss.

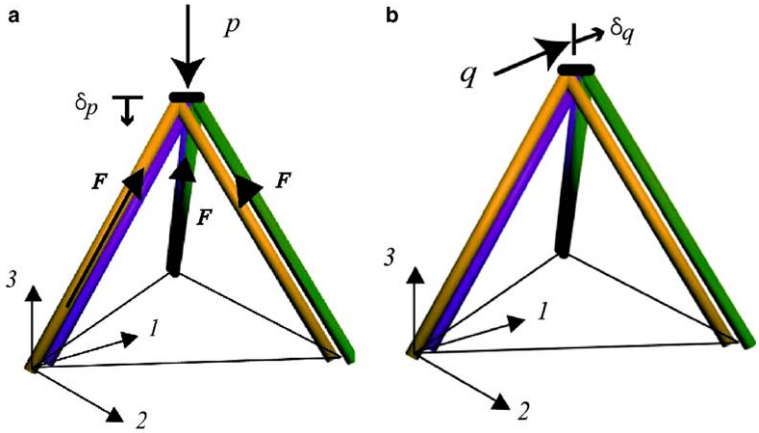

Fig. 5. Configurations of tetrahedral truss with each struts having two wires: (a) under compression and (b) under shear force.

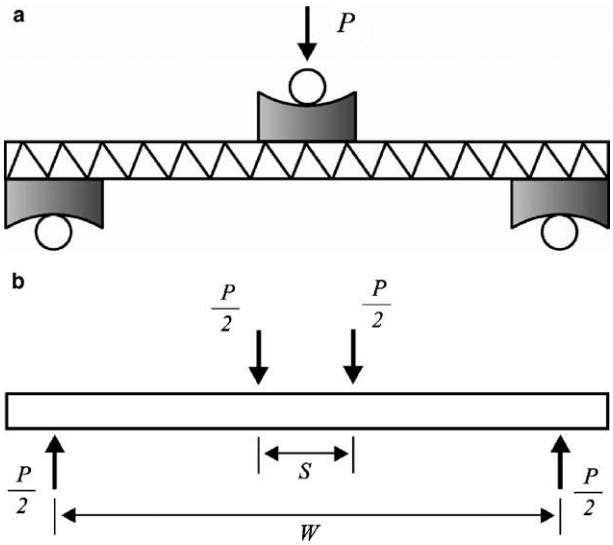

Fig. 6. (a) Configuration of three-point bending test and (b) equivalent free body diagram.

will be mentioned later.) Therefore, to take into account the significant width of the center block, the loading configuration is simulated by a four-point bending with the external force, P, replaced with two $P/2$'s separated by the width of block, S, as shown in Fig. 6(b). Referring to Allen (1969), the compliance is given by

$$\frac{\delta}{P} = \frac{(W-S)^2(W+2S)}{48(EI)_{\mathrm{eq}}} + \frac{(W-S)}{4(AG)_{\mathrm{eq}}}, \tag{4}$$

where δ is deflection at the center due to P and W is the span between the two rollers. And $(EI)_{\mathrm{eq}}$ and $(AG)_{\mathrm{eq}}$ are equivalent bending and shear rigidity, respectively, given by

$$(EI)_{\mathrm{eq}} \approx \frac{E_{\mathrm{f}}^{\mathrm{eff}} B t_{\mathrm{f}} D^2}{2}, \qquad (AG)_{\mathrm{eq}} \approx G_{13} B D, \tag{5}$$

$E_{\mathrm{f}}^{\mathrm{eff}}$ is the effective Young's modulus of the face sheet. For the solid face sheet, $E_{\mathrm{f}}^{\mathrm{eff}}$ is the Young's modulus of the material itself, $E_{\mathrm{f}}^{\mathrm{eff}} = E_{\mathrm{f}}$. For the perforated face sheet, $E_{\mathrm{f}}^{\mathrm{eff}} = \sqrt{3}\frac{w}{l}E_{\mathrm{f}}$ if $w \ll l$. B is the width of the sandwich panel.

The compressive strength is governed by the buckling of the strut of the cores. When a force, p, is applied on the top of the tetrahedral truss as shown in Fig. 5(a), the reaction force in each strut, F, is related with p by $p = \sqrt{6}F$. Considering that each strut is composed of two wires and assuming pin joints at the ends, the critical force, F_{c1}, and stress, σ_{c1}, corresponding to elastic buckling are,

$$F_{\mathrm{c1}} = \frac{\pi^2 E_{\mathrm{c}} I}{l^2}, \qquad \sigma_{\mathrm{c1}} = \frac{2F_{\mathrm{c1}}}{\pi d^2}, \tag{6}$$

where I is the second area moment of inertia of the strut, i.e., $I = \pi d^4/32$ (Bleich, 1952). If the critical stress, σ_{c}, is higher than the yield stress of the material, the strut buckles inelastically before elastic buckling. In the case, the critical force, F_{c2}, and stress, σ_{c2}, corresponding to inelastic buckling are

$$F_{\mathrm{c2}} = \frac{\pi^2 E_{\mathrm{ct}} I}{l^2}, \qquad \sigma_{\mathrm{c2}} = \frac{2F_{\mathrm{c2}}}{\pi d^2}, \tag{7}$$

where E_{ct} is the tangential modulus of the material, that is, the slope of the stress–strain curve after yielding, defined as $E_{\mathrm{ct}} = \mathrm{d}\sigma/\mathrm{d}\varepsilon$.

According to Wicks and Hutchinson (2001, 2004), when a sandwich panel is under bending load, it has four failure modes: face yielding, buckling of one of the face sheets, core yielding, and buckling of struts in the core. If the thickness of the face sheets is so thin that the face sheets fail by buckling, the maximum load, $P_{\max}$, corresponding to buckling of one of the face sheets is,

$$\frac{P_{\max}}{B} = \left(\frac{4}{W-S}\right)\frac{D}{l}F_{\mathrm{f}}, \tag{8}$$

where F_{f} is the buckling load of the face sheet itself per a single bar length in the direction of width. If the slenderness of the strut is so high that the struts fail by buckling, the maximum load, $P_{\max}$, corresponding to buckling of the struts is

$$\frac{P_{\max}}{B} = \frac{2}{l}\frac{D}{l}F_{\mathrm{c}}, \tag{9}$$

where F_{c} is the buckling load of the strut given by Eq. (6) or (7). In the case that the panel has the perforated face sheets, $F_{\mathrm{f}} \approx F_{\mathrm{c}}$. Then, from comparison between Eqs. (8) and (9), the sandwich panel may fail due to the buckling of the face sheet, to be more specific, the buckling of a row of bars of face sheets, which will be shown later. On the other hand, when $F_{\mathrm{f}} \gg F_{\mathrm{c}}$, the sandwich panel fails due to the buckling of the struts in the core.

Table 1
Dimensions of the sandwich panel specimen for bending test

Size (mm)	Tetrahedral		Kagome
	Perforated face sheet	Solid face sheet	Perforated face sheet
d	0.9		0.5
l	20		20
t_f	0.8		0.6
w	1.55		2
D	16.33		18.5
S	30		30
L	263	267	320
W	233	237	290
B	113	118	96

Low carbon steel wires with a diameter of $d = 0.9$ mm were the raw material of the core. The length of strut was $l = 20$ mm. The thickness of face sheets, w was $t_f = 0.8$ mm, and the in-plane thickness of bars composing the perforated face sheets was designed so that the bars could have the same I as the strut of the core, i.e., two wires, $w = 1.55$ mm. The overall dimension of the panel for bending tests was about 265 mm in length × 115 mm in width × 16 mm in thickness, which accommodated 15 trusses in length, and $5\frac{1}{2}$ trusses in width. The detailed dimensions are listed in Table 1. The dimensions of specimens for compression tests were the same as those for bending tests except for the length of panel, changed to $L = 120$ mm, which accommodated six trusses in length.

The material of the face sheets was also a low carbon steel JIS SS41. Laser cutting was employed to make the perforations. A simple press was used to bend the wires into the triangular wave shape as shown in Fig. 2(a). Then, the wires were manually assembled into the tetrahedral truss shaped core as described in Fig. 2(b)–(d). Some of the apices were bound at with thin copper wires to keep the shape. To bond the core with the face sheets, the core was assembled with the face sheets on the top and bottom, and copper paste was injected at every contact point. Then, finally, the assembly with carbon blocks on the top and bottom was put on the gas furnace conveyor moving at 180 mm/min and was heated up to 1172 °C and cooled down in the oxygen-free environment. The brazing lasted a total of 2 h.

2.2. Kagome truss core sandwich panel

Fig. 1(b) shows a typical sandwich panel with the Kagome truss core. An approach similar to that of the tetrahedral truss was applied to form the core. First, wires were bent into the trapezoidal wave shape shown in Fig. 7(a), and then, were assembled together as shown in Fig. 7(b)–(d). Each strut was composed of two twisted wires. At each top and bottom of the assembly, three wires were made into a regular triangle, which looks like the trigonal pyramid with the apex cut. At the middle plane, six wires were bent slightly so that they could pass by each other at a point (see the right insets in Fig. 7(d) for enlarged images). Fig. 8 is a top view of Fig. 7(d). Each point where the six wires met had twisted struts, and one wire of the strut hid beneath the other and three wires overlapped each other clockwise (or counter-clockwise). Finally, two face sheets were bonded on the top and bottom of the truss core to form a sandwich panel.

The theoretical relative density, strength, and stiffness of the panel were similar in form to those of the panel with the tetrahedral truss. Fig. 9 illustrates the perforated face sheet, which had a two-dimensional Kagome truss pattern (Hyun and Torquato, 2002). If the material of the face sheets is the same as that of the core, the relative density of the panel with the perforated face sheet and the one with the solid face sheet are

$$\rho = \frac{6\sqrt{2}wt_f}{l^2} + \left(\frac{3}{2}\right)\frac{3\sqrt{2}}{\pi d^2}2l^2 \quad \text{and} \quad \rho = \frac{\sqrt{6}t_f}{l} + \left(\frac{3}{2}\right)\frac{3\sqrt{2}\pi d^2}{2l^2}, \tag{10}$$

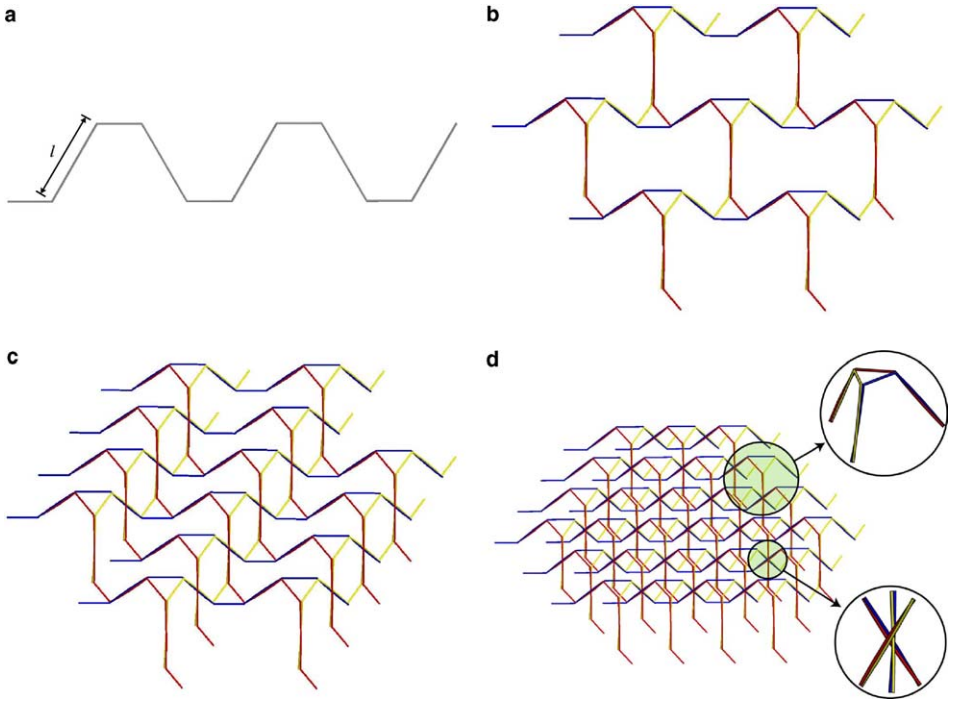

Fig. 7. Fabricating process of Kagome sandwich panel with wires: (a) unit wire composing the truss, (b) quarter structure for Kagome truss core, (c) half structure for Kagome truss core, (d) fully assembled truss, where the upper inset shows how to form Kagome truss core and the low inset indicates that each strut is composed of two twisted wires.

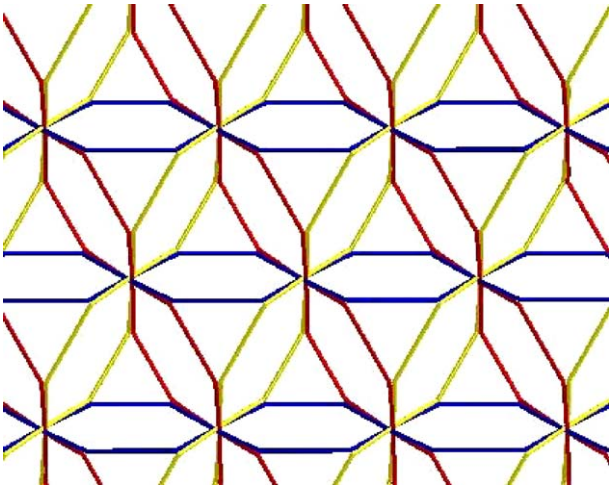

Fig. 8. Top view of the Kagome core shown in Fig. 7.

respectively, where l is defined as the length of the inclined part of the wire, as indicated in Fig. 7(a). Compared with Eq. (1) for the tetrahedral truss panel, the second terms in Eq. (10) are increased by

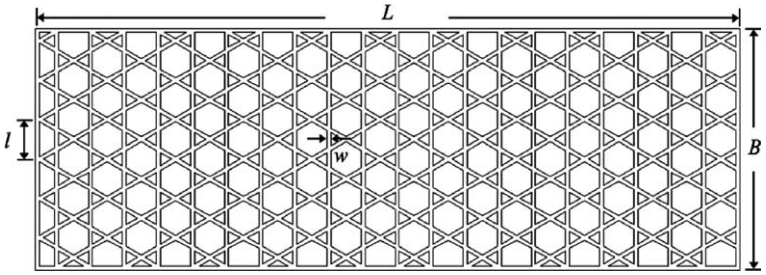

Fig. 9. Configuration of a perforated face sheet for the Kagome truss.

50% due to the part of wires on the top and bottom of the core where the wires directly contacted the face sheets. See the right insets of Fig. 7(d).

By similar argument to that in the preceding section, the stiffness, p/δ_p, q/δ_q, and effective elastic moduli, E_{33} and G_{13}, are given by the same equations, i.e., Eqs. (2) and (3), respectively. And the compliance under bending load is also given by Eq. (4).

Because the length of struts in the Kagome truss was half of that of the tetrahedral truss, $l/2$, Eqs. (6) and (7) for the buckling strength of the strut should be modified. That is, the critical force, F_{c1}, and stress, σ_{c1}, corresponding to elastic buckling are

$$F_{c1} = \frac{4\pi^2 E_c I}{l^2}, \qquad \sigma_{c1} = \frac{2F_{c1}}{\pi d^2}. \tag{11}$$

The critical force, F_{c2}, and stress, σ_{c2}, corresponding to inelastic buckling are

$$F_{c2} = \frac{4\pi^2 E_{ct} I}{l^2}, \qquad \sigma_{c2} = \frac{2F_{c2}}{\pi d^2}. \tag{12}$$

When the sandwich panel with the Kagome truss core is under bending load, the maximum allowable load, P_{max}, for buckling of one of the face sheets and that for the buckling of the struts are still given by Eqs. (8) and (9), respectively. However, F_c in Eq. (9), i.e., the critical buckling force of a single strut, is given by Eq. (11) or (12). On selection of the two buckling failure modes, the same argument as that for the tetrahedral truss would be valid.

Zinc-plated copper wires with a diameter of $d = 0.5$ mm served as the raw material of the core. The length of the strut was $l/2 = 10$ mm. The thickness of face sheets was $t_f = 0.6$ mm and the in-plane thickness of bars composing the perforated face sheets was $w = 2$ mm. The overall dimensions of the panel for bending tests were about 320 mm in length × 96 mm in width × 18.5 mm in thickness, which accommodated 20 trusses in length and 5 trusses in width. The detailed dimensions are listed in Table 1. The dimensions of the specimens for compression tests were the same as those for bending tests, except for the length of the panel which changed to $L = 123$ mm, which accommodated six trusses in length.

The material of the face sheets was low carbon steel JIS SS41. The bars composing the perforated face sheet have much higher strength and bending modulus, EI, than the struts of cores, made of the thin copper wires. Consequently, even the panels with the perforated face sheets were expected to fail due to buckling of the struts in the core. And only the panels with the perforated face sheets were fabricated in this work. Laser cutting was employed to make the perforations. A simple press was used to bend the wires into the trapezoidal wave shape as shown in Fig. 7(a). Then, the wires were manually assembled into Kagome truss shaped cores as described in Fig. 7(b)–(d). Manual electric soldering was employed to fix the core at the intersecting points at the middle plane and to bond the core with the face sheets. First, the wires were assembled on the lower face sheet, and then, the whole assembly was turned over and were put on the other face sheet and bonded along the contact lines.

3. Experiments and the results

First, tensile tests were performed to obtain the material properties of the wires. The specimen length, i.e., the distance between the upper and lower grips, was 150 mm. The strain was measured by an extensometer with the gage length of 25 mm. The rate of displacement was controlled to 0.05 mm/s. Next, compression tests and bending tests for the sandwich panels with the tetrahedral truss and Kagome truss cores fabricated from the wires were carried out. The displacement rate for the tests was even more slowly controlled to 0.01 and 0.02 mm/s, respectively. All tests were performed on an electric–hydraulic material test machine, INSTRON 8800. The behavior of the specimens during the compression and the bending tests were monitored by two digital cameras, Kodak Megaplus ES 1.0.

3.1. Tetrahedral truss core sandwich panel

The Young's modulus of the steel wire put into the brazing furnace and heat-treated together with the sandwich panels was $E_c = 193$ GPa. The yield stress was $\sigma_y = 170.9$ MPa, which was significantly lower than that of the untreated wires, $\sigma_y = 250$–300 MPa. The exposure of the wires to the high temperature during brazing accounted for the lower yield stress. Fig. 10 shows the stress–strain relation after yielding during the tensile test, which was used to evaluate the inelastic buckling strength of the struts.

Fig. 11 shows the load–displacement curve during the compression test. After the maximum point, the load drops rapidly. The recorded video images revealed that all the tetrahedral trusses suddenly buckled at this point. The stiffness calculated from the slope of the linear portion just before the maximum point in the load–displacement curve is $(P/\delta_p)_{comp} = 795.2$ kN/mm. For a single truss, the stiffness is estimated by Eq. (2) as $p/\delta_p = 25.2$ kN/mm and is multiplied by the number of trusses in the compressive specimen, $N = 5.5 \times 6 = 33$, to yield $(P/\delta_p)_{comp} = 841.5$ kN/mm, which is about 6% over-estimation. The measured maximum load was $(P_{max})_{comp} = 14.7$ kN. Because the critical stress corresponding to elastic buckling of a single strut was higher than the material yield stress (strictly speaking, the proportional limit), the maximum load can be estimated from Eq. (7) for inelastic buckling and the stress–strain relation shown in Fig. 10, which gives $(P_{max})_{comp} = 17.8$ kN, which is about 21% over-estimation.

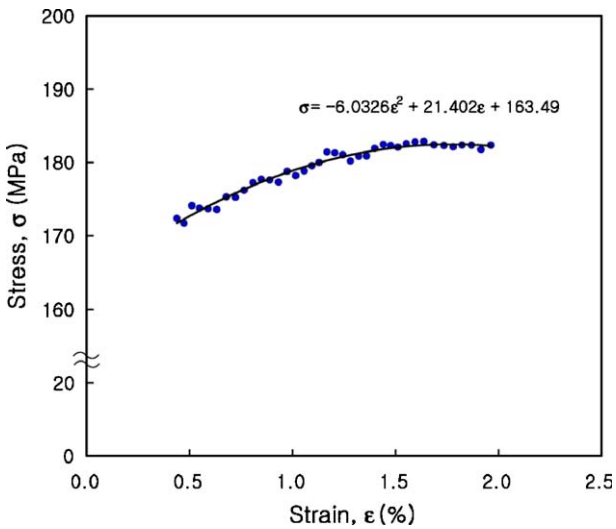

Fig. 10. Enlarged view of stress–strain relationship after yielding during the tensile test of steel wire for tetrahedral truss core.

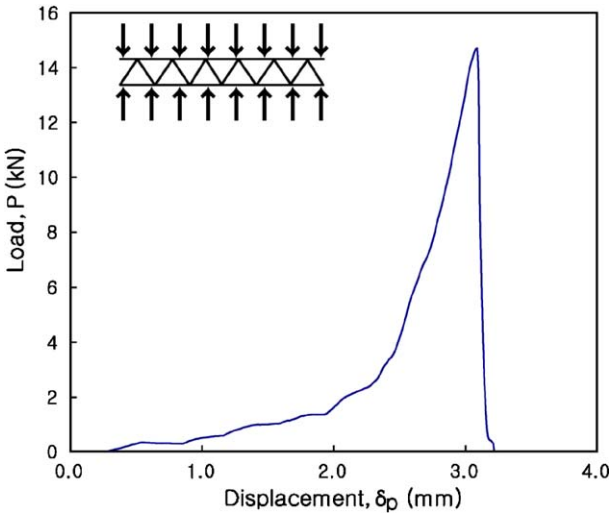

Fig. 11. Compressive response of the tetrahedral sandwich panel.

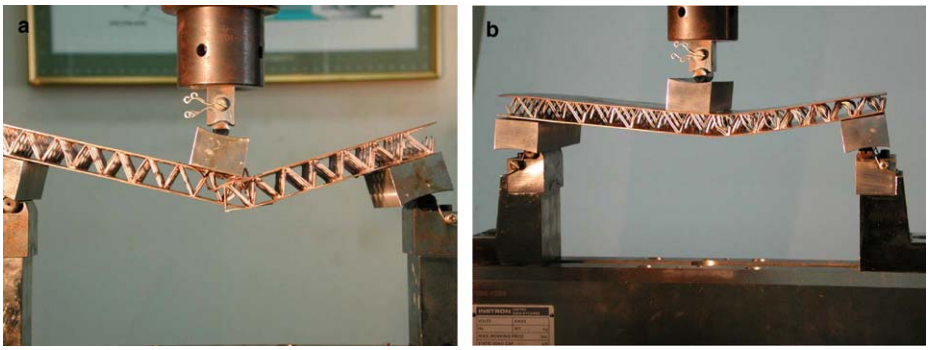

Fig. 12. Images showing the buckled tetrahedral sandwich panels after three-point bending test (a) with perforated face sheets and (b) with solid face sheets.

Fig. 12 shows the deformed shape of the sandwich panel after the peak load of the bending test. As predicted, the panel with the perforated solid face sheets failed due to the local buckling at a few bars of the upper face sheet near the center block (Fig. 12(a)), while the one with the solid face sheets failed due to buckling of the truss core in the right half of the span (Fig. 12(b)). Brazed joints did not break. Fig. 13 shows the load–displacement curves of the bending test. Regardless of whether the face sheets were perforated (Fig. 13) or solid (Fig. 13), the load dropped rapidly after the peak because of the unstable failure mechanism, that is, the buckling, as shown in Fig. 12. However, after the load dropped to the 55% level of the peak load, the load level remained almost constant for the panel with the perforated face sheets, while it continued to decrease to the 23% level of the peak load for the panel with the solid face sheets. The bending stiffness measured from the initial linear portion in the load–displacement curves was $(P/\delta)_{\text{bend}} = 1.24$ kN/mm and $(P/\delta)_{\text{bend}} = 3.78$ kN/mm for the panels with the perforated and the solid face sheet, respectively. Compared with $(P/\delta)_{\text{bend}} = 1.45$ kN/mm and $(P/\delta)_{\text{bend}} = 4.7$ kN/mm estimated by using Eqs. (4) and (5), the measured stiffnesses were lower by about 14% and 20%, respectively. The measured

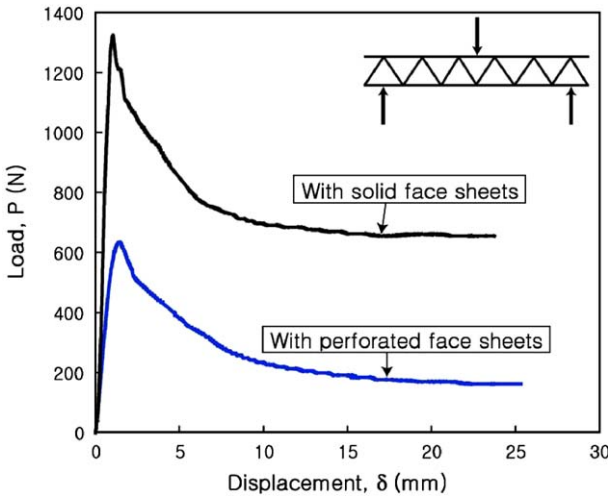

Fig. 13. The three-point bending responses of the tetrahedral sandwich panels with perforated and solid face sheets.

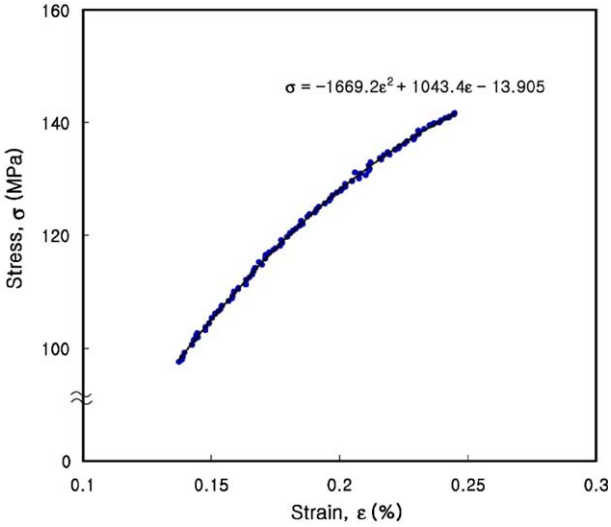

Fig. 14. Enlarged view of stress–strain relation after yielding during the tensile test of copper wire for Kagome truss core.

maximum loads were $(P_{\max})_{\text{bend}} = 0.63$ kN and $(P_{\max})_{\text{bend}} = 1.32$ kN for the panels with the perforated and the solid face sheet, respectively. For the two types of panels, the estimated maximum loads were based on Eqs. (8) and (9) together with Eq. (7) for the critical load for inelastic buckling, which yielded $(P_{\max})_{\text{bend}} = 0.98$ kN and $(P_{\max})_{\text{bend}} = 1.62$ kN, which were about 36% and 19% over-estimation, respectively.

3.2. Kagome truss core sandwich panel

The Young's modulus of the copper wire was $E_c = 102$ GPa. The yield stress was $\sigma_y = 98$ MPa. Fig. 14 shows the stress–strain relation after yielding in the tensile test, which was used to evaluate the inelastic buckling strength of the struts.

Fig. 15 shows the load–displacement curve of the compressive test. After the maximum load, the load drops rapidly in the similar way as shown in Fig. 11 for the panel with the tetrahedral truss core. However, when the load reaches about half of the maximum load, it increases again until it reaches about the 30% higher load level. The double peaks in the load–displacement curve have never been reported. The recorded video images reveal a peculiar pattern of truss deformation. Fig. 16 shows a series of the pictures of local deformation during compression. Notice that all the struts in the pictures are not straight, but bent a little so as to pass by each other at the middle plane as mentioned earlier. Until the maximum load was attained, the truss cores appeared to keep the initial shape (Fig. 16(a) and (b)). After the maximum, ones of the upper and lower tetrahedral composing a Kagome truss buckled and continued to deform with the load level decreased as the compression proceeded, while the shape of the others remained unchanged. See the bold circles indicating the buckling in Fig. 16(c). After more compression, the deformation reached to the limit, then the rest tetrahedral began to resist the compression, which increased the load level again. Finally, after the second peak, the rest buckle and then the load level decreased. The stiffness calculated from the slope of the initial linear portion in the load–displacement curve was $(P/\delta_p)_{\text{comp}} = 71.8$ kN/mm. For a single truss, the stiffness was estimated by Eq. (2) as $p/\delta_p = 4.01$ kN/mm and it was multiplied by the number of trusses in the compressive specimen, $N = 5 \times 6 = 30$, which yielded $(P/\delta_p)_{\text{comp}} = 120.17$ kN/mm, which was about 67% over-estimation. The large error seemed to be due to the non-flat contact between the specimen and grip. The measured maximum load was $(P_{\max})_{\text{comp}} = 2.33$ kN. Because the critical stress corresponding to elastic buckling of a single strut was higher than the material yield stress, the maximum load was estimated based on Eq. (7) for inelastic buckling and the stress–strain relation shown in Fig. 14, which gave $(P_{\max})_{\text{comp}} = 2.97$ kN, which was about 27% over-estimation.

Fig. 17 shows the deformed shape of the sandwich panel after the peak load during the bending test. As predicted, even though the panel had the perforated face sheets, it failed due to buckling of the truss core. Note that the buckling occurred only in half of the length. The soldered joints did not break. Fig. 18 shows the load–displacement curves during the bending test. Contrary to the panel with the tetrahedral truss core, the load did not drop so rapidly after the peak. The bending stiffness measured from the initial linear

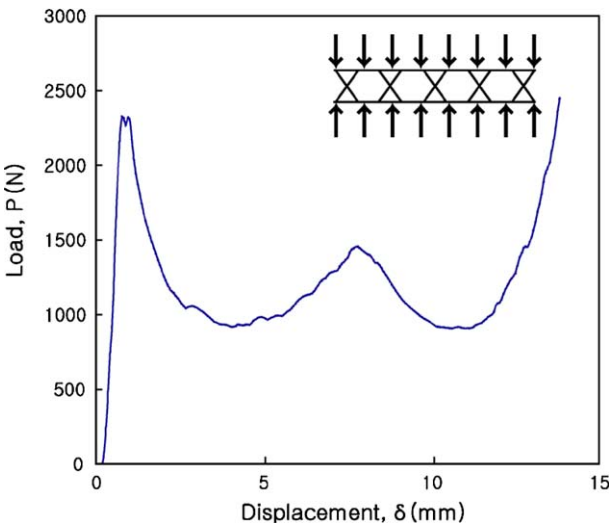

Fig. 15. Compressive response of the Kagome sandwich panel.

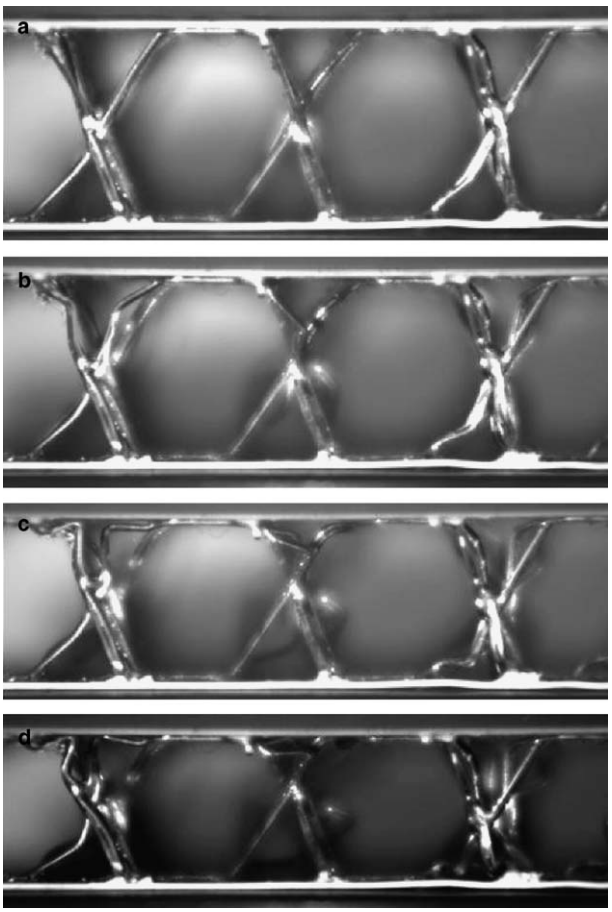

Fig. 16. Images of the Kagome sandwich panel during compression test.

portion in the load–displacement curves was $(P/\delta)_{\text{bend}} = 0.38$ kN/mm. Compared with $(P/\delta)_{\text{bend}} = 0.49$ kN/mm estimated by using Eqs. (4) and (5), the measured ones were about 29% lower. The measured maximum loads were $(P_{\max})_{\text{bend}} = 0.46$ kN. The maximum load was estimated based on Eq. (9) together with Eq. (7) for the critical load for inelastic buckling, which yielded $(P_{\max})_{\text{bend}} = 0.39$ kN, which was about 15% under-estimation.

4. Discussion

All the results on relative density, stiffness, and strength under bending and compression measured by experiments and estimated by Eqs. (1)–(12) are listed in Table 2. The relative density of the panel with the Kagome truss core was calculated under the assumption that the material of the face sheets was the same as that of the cores. Therefore, the relative density can be regarded as the volume occupancy, that is, 1-*porosity*. In the table, all the estimated results of the strength and stiffness are higher than the measured ones, except one. The over-estimations are attributed to the two sources. First, two parallel wires compos-

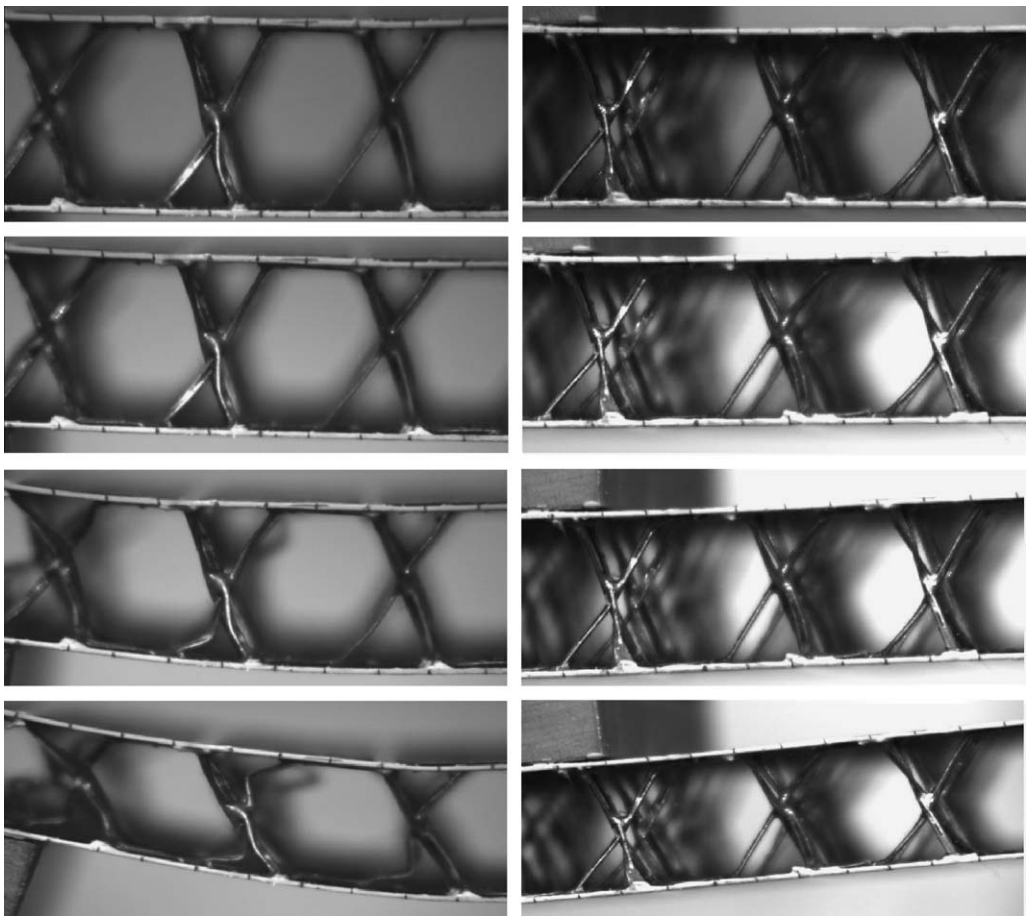

Fig. 17. Images of the Kagome sandwich panel during three-point bending test.

ing each strut in the tetrahedral trusses were often easily debonded from each other due to poor permeation of the brazing metal (copper) and buckled separately when the strut was under compression. Fig. 19 shows an enlarged view of the buckled wires in the compressive test, in which most of wires are separate. The debonding seems to result in the low buckling strength even though the exact reason has not been clearly addressed, yet. Second, on the middle plane of Kagome truss core, six wires have to be bent so as to pass by each other at a point; that is, the struts are not straight (see Fig. 16(a)). Consequently, the buckling strength reduces.

The only one exception to the over-estimations is the bending strength of the panel with Kagome truss core. The bending strength was estimated by Eq. (9), which stands under the assumption that the shear load is sustained by only the core struts and the contribution by the face sheets is negligible. However, the perforated sheets of the sandwich panel were made of thicker and stronger metal (steel, the cross section area of the bars composing the face sheets is 0.6 mm $\times$ 2 mm) than the core (copper, the diameter of the struts is 0.5 mm). Therefore, it seems arguable that the shear load sustained by the face sheets is not negligible, so the bending strength is underestimated. In conclusion, regardless of the overestimations or underestimation, the equations can be considered to give fairly good estimation on the stiffness or strength of the panels under compression and bending, if the theoretical simplicity is taken into account.

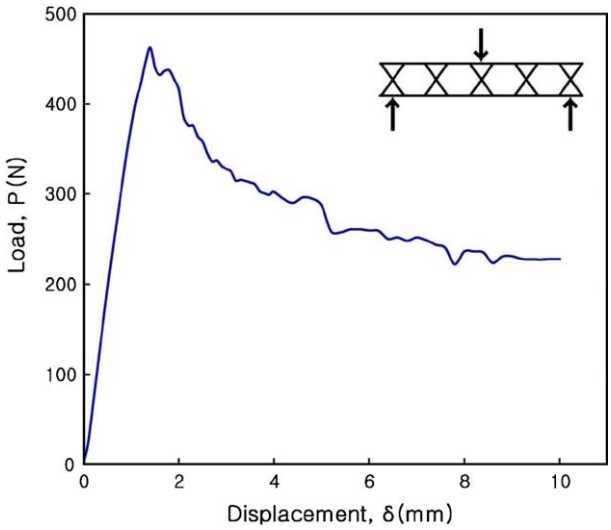

Fig. 18. The three-point bending responses of the Kagome sandwich panel.

Table 2
Relative density, stiffness and strength estimated by Eqs. (1)–(12) in comparison with measured ones

		Truss core and face sheet type		Theory (A)	Measured (B)	Error (%) $\left(\frac{A-B}{B}\times 100\right)$
ρ_{rel}		Tetrahedral core	Perforated	0.04	0.043	−7
			Solid	0.1115	0.114	−2
		Kagome		0.0317	0.036	−12
Stiffness (P/δ_p) [kN/mm]	Compression	Tetrahedral		841.5	795.2	6
		Kagome		120.17	71.8	67
	Bending	Tetrahedral core	Perforated	1.45	1.24	14
			Solid	4.7	3.78	20
		Kagome		0.49	0.38	29
Strength (P_{max}) [kN]	Compression	Tetrahedral		17.8	14.7	21
		Kagome		2.97	2.33	27
	Bending	Tetrahedral core	Perforated	0.98	0.63	36
			Solid	1.62	1.32	19
		Kagome		0.39	0.46	15

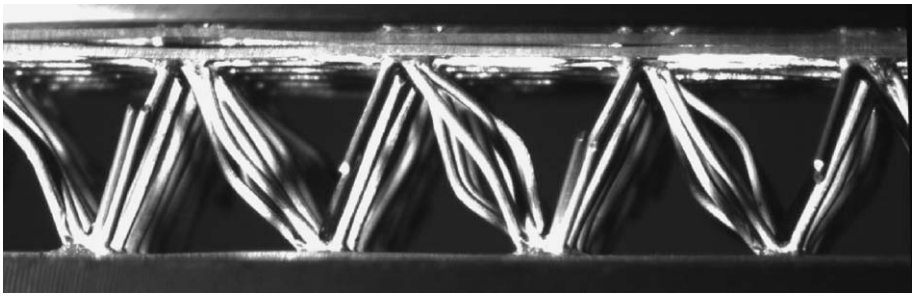

Fig. 19. Enlarged view of the buckled tetrahedral truss core after compression test.

All the specimens tested in this work failed by the plastic buckling of truss members, i.e., the core struts or the bars of face sheets. The plastic buckling is attributed to two sources as follows. First, the truss members had high slenderness. The struts of tetrahedral and Kagome truss had slenderness, $l/r = 89$ and $l/2r = 80$, respectively (r is radius of gyration of the cross section of the struts). Second, the material of the struts had high ductility and low yield stress. The materials were fully annealed low carbon steel and copper, which are used for electric wires. The yield stresses were 170.9 and 98 MPa, respectively, which led to the early plastic buckling before elastic buckling despite of the high slenderness of the truss members. Moreover, the wrought nature of the materials prevented brittle failure, which has been often found in truss of cast metals in previous works, as mentioned in Section 1. If, after brazing, the wires can be hardened through heat treatment like steel alloy that is quenched or an aluminum alloy that is aged, early plastic buckling will not occur, and the strength of the entire panel will be enhanced.

As shown in Figs. 11 and 15, the two kinds of sandwich panels behave drastically differently under compressive loading. The panel with the tetrahedral truss core shows a sharp drop in the load level after the peak load, while the one with Kagome truss core shows double peaks with a larger displacement. The latter implies a higher capacity of energy absorption. Some mechanical parts like a bumper of an automobile are designed to have a limit in the load capacity. The parts are not to deformed at all for a load level under the limit, but they are deformed for a load level over the limit and absorb the applied energy as much as possible. The panel with Kagome truss core seems to have high potential to be used for such parts. On the other hand, both panels behave similarly under the bending load, as long as the face sheet does not buckle. After the peak, the load level decreases stably and gradually approaches a relatively high level. For a while, plastic buckling occurs only in half of the span because of the shear strength of the tetrahedral truss depends on the orientation of the truss (Chiras et al., 2002). Even though the Kagome truss does not depend on its orientation, once buckling occurs in one half of the span, its shear strength decreases and more deformation occurs only in this half of the span. Similar asymmetry has also been observed in the Kagome panels of cast Cu–2%Be alloy (Wang et al., 2003). Both panels showed no local thinning.

Because the wires in the tetrahedral truss exhibited little interference with each other, as shown in Figs. 2 and 3, the struts with low slenderness (i.e., thick wires and short struts) could be easily made for heavy load applications. On the other hand, as shown in Fig. 7, the wires in Kagome truss should be bent near the middle plane of the core; therefore, the thicker the wire is, the harder it is to manage. Also the buckling strength would be deteriorated.

From the view point of production engineering, both methods would be good alternatives to previous methods for fabrication of trusses. Wires are easy to handle and the manufacturing process would be easy to construct with modern weaving technologies. The tetrahedral truss, especially, can be made simply by the tri-axial weaving and crimping process. Furthermore, wires have high strength with good quality and few flaws.

5. Conclusion

New approaches based on tri-axial weaving of wires to create ideal trusses, i.e., tetrahedral and Kagome truss, have been presented. The mechanical properties of sandwich panels with the truss cores fabricated by using the new approaches under compression and bending load are analyzed by elementary beam theory and experiments. As the results, the conclusions have been obtained as follows:

(i) The relative density, stiffness, and strength estimated by the equations agree with the measured results fairly well.

(ii) Regardless of the mode of loading, all the panels fail by the plastic buckling of the truss members, i.e., the struts of the core or the bars of the face sheet, because of the high slenderness of the truss members and the ductility and low yield stress of the material.
(iii) The first method, in which the tetrahedral truss core is fabricated from wires, appears to have advantage with respect to mass production and little interference among wires, which makes it possible to achieve struts with low slenderness. And also the truss made by the first method has the lower relative density for a given stiffness and strength than the one made by the other method.
(iv) Under compression, Kagome truss core fabricated from wires by the second method exhibits double peaks on the load–displacement curve, a characteristic which makes it possible to absorb much more energy during deformation.

Acknowledgements

The authors thank Prof. A.G. Evans for initial inspiration and helpful discussion. Funding for this work was provided by Hyundai Motors through the project for Next Generation Vehicles, 2003.

References

Allen, H.G., 1969. Analysis and Design of Structural Sandwich Panels, first ed. Pergamon Press, New York.
Bleich, F., 1952. Buckling Strength of Metal Structures. McGraw-Hill, New York.
Chiras, S., Mumm, D.R., Wicks, N., Evans, A.G., Hutchinson, J.W., Dharamasena, K., Wadley, H.N.G., Fichter, S., 2002. The structural performance of near-optimized truss core panels. International Journal of Solids and Structures 39, 4093–4115.
Deshpande, V.S., Fleck, N.A., 2001. Collapse of truss core sandwich beams in 3-point bending. International Journal of Solids and Structures 38, 6275–6305.
Deshpande, V.S., Fleck, N.A., Ashby, M.F., 2001. Effective properties of the octet-truss lattice material. Journal of the Mechanics and Physics of Solids 49, 1747–1769.
Gere, J.M., 2001. Mechanics of Material, fifth ed. Brooks/Cole, Belmont, CA.
Hyun, S., Torquato, S., 2002. Optimal and manufacturable two-dimensional, Kagomé-like cellular solids. Journal of Materials Research 17, 137–144.
Hyun, S., Karlsson, A.M., Torquato, S., Evans, A.G., 2003. Simulated properties of Kagome and tetragonal truss core panel. International Journal of Solids and Structures 40, 6989–6998.
Jung, J.G., Yoon, S.J., Sung, T.Y., Yang, D.Y., Ahn, D.G., 2004. Ultra light inner structured and bonded metal panel made of the metallic pyramidal structure. Proceeding of Spring Meeting of Korean Society of Precision Engineering, 928–931.
Queheillalt, D.T., Wadley, H.N.G., 2005. Cellular metal lattices with hollow trusses. Acta Materialia 53, 303–313.
Rathbun, H.J., Wei, Z., He, M.Y., Zok, F.W., Evans, A.G., Sypeck, D.J., Wadley, H.N.G., 2004. Measurement and simulation of the performance of a lightweight metallic sandwich structure with a tetrahedral truss core. Journal of Applied Mechanics 71, 368–374.
Sugimura, Y., 2004. Mechanical response of single-layer tetrahedral trusses under shear loading. Mechanics of Materials 36, 715–721.
Sypeck, D.J., Wadley, H.N.G., 2001. Multifunctional microtruss laminates: textile synthesis and properties. Journal of Materials Research 16, 890–897.
Sypeck, D.J., Wadley, H.N.G., 2002. Cellular metal truss core sandwich structures. Advanced Engineering Materials 4, 759–764.
Wadley, H.N.G., 2002. Cellular metals manufacturing. Advanced Engineering Materials 4, 726–733.
Wadley, H.N.G., Fleck, N.A., Evans, A.G., 2003. Fabrication and structural performance of periodic cellular metal sandwich structures. Composites Science and Technologies 63, 2331–2343.
Wallach, J.C., Gibson, L.J., 2001a. Mechanical behavior of a three-dimensional truss material. International Journal of Solids and Structures 38, 7181–7196.
Wallach, J.C., Gibson, L.J., 2001b. Defect sensitivity of a 3D truss material. Scripta Materialia 45, 639–644.
Wallach, J.C., Gibson, L.J., 2003. Truss core sandwich panels and method for making same. US Patent 6,644,535 B2.

Wang, J., Evans, A.G., Dharmasena, K., Wadley, H.N.G., 2003. On the performance of truss panels with Kagome cores. International Journal of Solids and Structures 40, 6981–6988.
Wicks, N., Hutchinson, J.W., 2001. Optimal truss plates. International Journal of Solids and Structures 38, 5165–5183.
Wicks, N., Hutchinson, J.W., 2004. Performance of sandwich plates with truss cores. Mechanics of Materials 38, 739–751.
Zhou, J., Shrotriya, P., Soboyejo, W.O., 2004. On the deformation of aluminum lattice block structures: from struts to structures. Mechanics of Materials 36, 723–737.